LAT-TD-08777-03
An End-to-end test of GLAST LAT Absolute Timing

David A. Smith[1], J. Eric Grove[2], and Denis Dumora[1]

[1] *Université Bordeaux 1 and CNRS/IN2P3, Centre d'Etudes Nucléaires de Bordeaux Gradignan, UMR 5797, Chemin du Solarium, BP120, 33175 Gradignan, France* smith@cenbg.in2p3.fr

[2] *Naval Research Laboratory, Code 7650, 4555 Overlook Ave. SW, Washington, DC 20375 USA*

30 November 2006, update 11/12/06.

Abstract

We exploit the quasi-simultaneity of cosmic ray muons traversing both the GLAST LAT and an independent charged particle dectector to validate the absolute times recorded with the LAT. The particle detector is a muon telescope, made with scintillators and photomultiplier tubes, that latches UTC (Coordinated Universal Time) as determined by a GPS receiver in a VME data acquisition system. Measurements using the VSC (Virtual Space Craft) in place of GLAST to demonstrate proof-of-principle of the method yield a dispersion of 0.7 μs. An observed offset of 24 ms and a clock drift of 2.0083 μs/s are attributed to the VSC. If, as expected, the GLAST observatory has neither the offset nor the drift and preserves the low dispersion, timing performance will be more than adequate to measure accurate neutron star rotation phases for gamma rays arriving from pulsars.

1 Motivation and Method

Beginning in late 2007, the Large Area Telescope ("LAT") on the Gamma Large Area Space Telescope ("GLAST") satellite should record GeV gamma rays from scores to hundreds of rotating neutron stars ("pulsars") [1]. Pulsation studies require accurate gamma ray arrival times. The mission requirement is 10 μs relative to an *absolute* time reference such as UTC (Coordinated Universal Time) (see section 2.6 of [2]) [1].

Event time measurements have two main components:

1. The observatory (i.e., the spacecraft) uses GPS receivers to obtain absolute time in UTC. The spacecraft sends a "Time Tone Message" with a date as an integer number of seconds to the LAT. A PPS signal ("Pulse Per Second") from the observatory then marks the instant of that date. Section 3.2.5.4 of [3] states that the PPS shall be accurate to $\pm 0.5\,\mu$s. Section 3.2.5.7 further states that if the GPS signals are lost, that the PPS's shall drift no more than $\pm 0.01\,\mu$s per second. The observatory C&DH subsystem provides the TimeTone and PPS to the LAT ("Control & Data Handling", via the IEM="Instrument Electronics Module" crate).

2. The LAT determines event arrival times relative to the PPS signal using a 25-bit scaler to count the ticks of a (nominally) 20 MHz clock located in the GEM ("GLT Electronics Module", where GLT stands for Global Trigger). That is, 50 ns per tick, for a full scale of $2^{25} = 33,554,432$ ticks every 1.68 seconds. The number of GEM ticks at the PPS arrival time is stored, and is subtracted from the number of GEM ticks latched by an event trigger, to thus obtain the fraction of a second since the most recent pair of TimeToneMessage and PPS. Section 5.2.11 of [4] states "the time accuracy of event time measurements shall be $< 10\,\mu$s relative to spacecraft time [and] the goal is to achieve accuracy better than $2\,\mu$s".

Until integration of both the LAT and the C&DH subsystem onto the spacecraft, the VSC replaces the observatory (the "Virtual Spacecraft", [5]). The VSC PPS signals are inaccurate, because the VSC GPS is not connected to an antenna, yet allowed proof-of-principle tests of our method.

The timing chain is complex. Recent major astrophysics space missions have had absolute timing problems, amongst which are Chandra [7] and XMM [8]. Pre-launch identification of any GLAST LAT timing problems would ease mitigation. The present work describes a comparison

[1] Many details, data files, software, etc are provided at `http://confluence.slac.stanford.edu/display/CAL/Event+Timestamps`, referred to as the "Confluence Timing page" in the rest of this document.

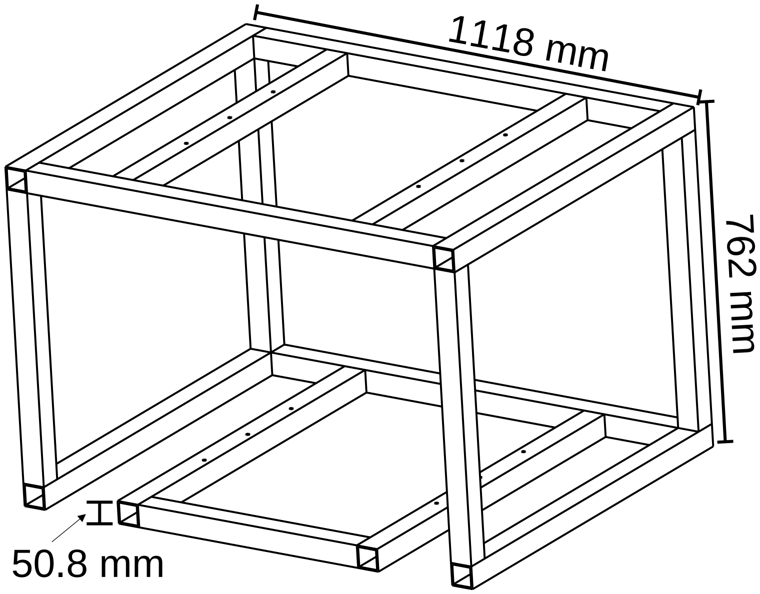

Figure 1: The scintillator paddle support stand for the muon telescope. Three screw-holes for the paddle support brackets are visible on four cross members. The phototube axes run parallel to the lines of holes, half-way between the cross members. The phototube bases extend beyond the long edge of the stand, hence the left-most (East) edge of the stand is placed next to the LAT. The top paddle is moved to extend beyond the left-most edge. Adapted from [10].

of GLAST LAT times with independent dating of quasi-simultaneous events, namely, the passage of cosmic ray muons through both the LAT and a simple "muon telescope" equipped with a GPS receiver. "Quasi" refers to the $\sim$ 10 ns transit time between the LAT tracker and the muon telescope, which we'll neglect from here on. The authors had both a muon telescope and a data acquisition system with GPS at hand, making the test preparations relatively simple.

2 Experimental Setup

A document describing how to set up the equipment and acquire data is available on the confluence web page.

2.1 Muon Telescope

Atmospheric muons ($\mu^{\pm}$ particles) come from the decay of $\pi^{\pm}$ particles produced high in the atmosphere in collisions of cosmic ray ions (mainly hydrogen, i.e. protons) with air molecules. Most muons with energy above $\sim$ 1 GeV reach the ground before decaying. Muons cause some ionization along their path but otherwise don't interact, and in particular buildings or other overburden decrease their flux only slightly. More details are at [9].

Figure 1 shows the aluminum stand that supports the scintillator paddles. The muon telescope was used during integration of the LAT calorimeter modules at the Naval Research Laboratory. It consists of 2 square plastic scintillators, 500 mm on a side and an inch thick. Each is equipped with two photomultipliers ("PMTs") on opposite sides. The two scintillators are housed in thin aluminum boxes, mounted on the stand [10]. The vertical separation of the scintillators is 711 mm. The relevant width is 1118 mm, that is, for the stand oriented with the PMTs away from the LAT. Thus the scintillator edge is $(1118 - 500)/2 = 309$ mm from the stand edge. The geometry is summarized in table 1.

Figure 2 shows the muon telescope at the Y^{-} side (West) of the LAT. The LAT is on the transport pallet frame and base assembly [11]. The stand was 1.5" from the pallet. With the two scintillators bolted one above the other, no muons from the LAT reach the telescope (right-hand of figure). Therefore we unbolted the top scintillator and moved it closer to the LAT (left-hand drawing). The paddles were centered in the X-direction.

A NIM electronics crate houses high voltage supplies for the PMTs. The signals from the PMTs

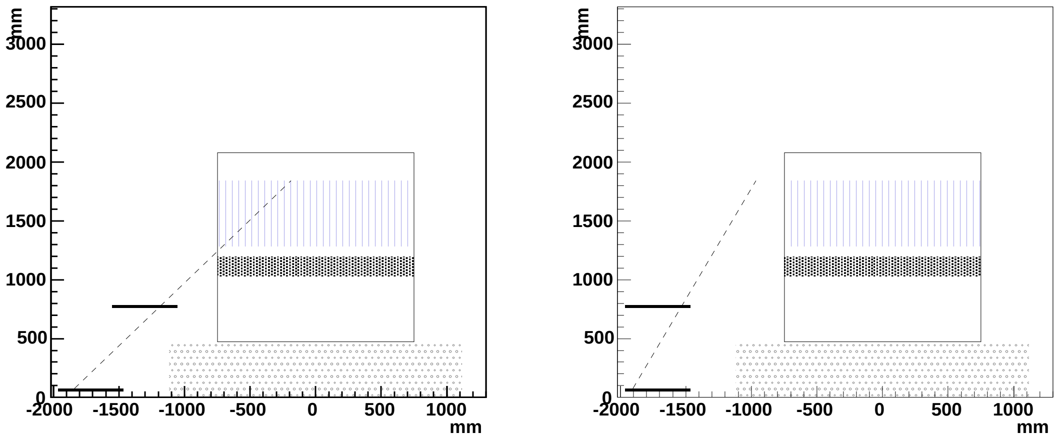

Figure 2: Muon telescope placement. Left: for run 77013003, with the top scintillator unbolted from the stand. Right: for runs '947, '948, '970. No coincidences were observed in data taken in this configuration.

are amplified, discriminated, and put into 4-fold coincidence using standard NIM electronics. The resulting trigger is fanned-out into two TTL signals and sent to the VME crate. Gate widths were a few hundreds of ns so that any ambiguity between rising and falling edges would induce a negligeable timing offset. The muon telescope triggered at 6 to 7 Hz with the two scintillators aligned vertically, and at 4.5 Hz when the top paddle was offset towards the LAT.

2.2 VME-based GPS Time Acquisition

This data acquisition system was used to search for 60 GeV gamma ray pulsars with the CELESTE experiment [14]. The accurate phases obtained for the Crab optical pulsar at different epochs over a few years prove the intrinsic accuracy of the equipment. The pulsar peak widths obtained with CELESTE in half-hour data runs were slightly larger than those measured by the best optical instruments, due to electronic sampling parameters, but allow us to assert that any clock drifts were smaller than those discussed later in this work.

A TTL trigger signal from the muon telescope latches the time measured with a Symmetricom TTM637VME GPS receiver [15]. This is the same module used in the Virtual Spacecraft [5]. Spectrum Astro provided a cable from the GPS antenna(s) on the roof the Factory of the Future. A second TTL trigger signal interupts the Motorola MVME172 crate controller, initiating readout of the GPS time.

Section 1.5.5 (page 1-9) of the TTM637 documentation [15] states that if the input time source of the TFP ("Time Frequency Processor") is lost, the internal VCXO ("Voltage Controlled Crystal Oscillator") will continue to "flywheel" at the last known code rate, with a typical accuracy (drift) of $0.5\,\mu$s per second. However, the TTM637 in the VSC does not receive GPS satellite signals and so its oscillator does not get disciplined to an absolute reference. Hence the VCXO could, in principle, be operating at some undefined frequency in its ± 30 ppm control range, that is, it may be found to drift within $\pm 30\,\mu$s per second.

Figure 3 shows measurements made in Bordeaux in November of the time differences from two VME GPS's triggered simultaneously with a pulse generator. One is a bc637 from CELESTE, and the other is a TTM637 loaned to us by SLAC. (The Symmetricom bc637 was superseded by the TTM637 in 2004 but is similar in many respects.) Each module was connected to a separate antenna. The differences are over a half μs for almost a minute, diminishing to 300 ns. Shipping problems limited the time that we had both modules and we were unable to perform a longer test of these relative time differences.

The *absolute* times recorded by our GPS's with times agree to better than a second with the times obtained from `http://nist.time.gov/timezone.cgi?UTC/s/0/java`. These two tests are currently our best evidence that we still provide stable absolute time stamps with this equipment.

Item	Height above floor (mm)	LAT Z-coordinate (mm)	Reference
Top of the LAT	2159 (a)	835 (814) (b)	See notes.
LAT coordinate origin	1324	0	(2083-835)
Highest silicon layer		595	[13]
Lowest silicon layer		42	[13]
Lower Paddle	64		[10]
Upper Paddle	774		[10]
Bottom of calorimeter	1105		[13]
Height of transport stand	471		[11]
		LAT Y-coordinate (mm)	
West edge of LAT pallet		-1118	[11]
West edge of active silicon		-741	[13]
East edge of telescope stand		-1156	[10]
East edge of lower scintillator		-1464	Note (c)
East edge of upper scintillator		-1054	Note (d)

Table 1: Summary of dimensions and positions for the test conducted before LAT integration onto the observatory. The X+ direction is South and the Y+ direction is East. Notes: a) M. Campbell, private communication. b) An event display was used to obtain the first value, extrapolating from the known Z-coordinates of the first and last tracker silicon layers. The 2^{nd} is more accurate [12], and will be used for tests with the spacecraft. c) The telescope stand was 1.5” from the transport pallet. d) The upper scintillator extended 4” over the edge of the stand.

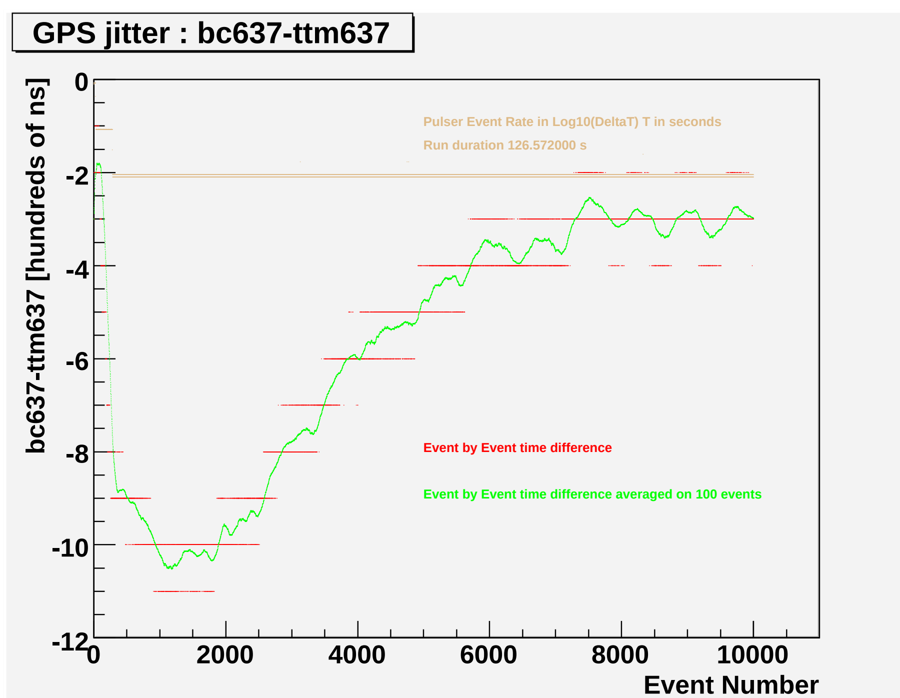

Figure 3: Differences in the times recorded with two independent VME GPS modules, a bc637 and a TTM637, both from Symmetricom, a few days prior to the first runs at the Factory of the Future. The former used a Trimble antenna, the latter interprets the GPS L1 signals on the VME board. Time agreement improved from 1 μs to 0.3 μs over the 2 minute data run.

LAT run	Standalone file	Comment
77012947	SASS8.dat	Vertical telescope configuration.
77012948	SASS9.dat	Ditto.
77012970	SASS10.dat	Ditto.
77013002	SASS11.dat	Telescope even farther from LAT.
77013003	SASS12.dat	Top paddle moved closer to LAT.

Table 2: The 5 data sets acquired Wednesday through Saturday, November 16 to 18, 2006. Only the last run uses the favorable geometry shown in figure 2 and has muon coincidences between the LAT and the telescope. LAT muon data rates are 490 Hz and each half-hour run contains about $880,000$ events. The standalone VME GPS runs contain about $10,000$ events each, taken concurrently with the LAT runs.

2.3 Data Reduction

Table 2 lists the data runs taken. Only the pair 77013003/SASS12 contains useful coincidences and the others will be disregarded.

Once acquired, the LAT data is automatically transferred to the SLAC computer center and "reconstructed". For the purposes of this work, that means that a straight line corresponding to the muon trajectory through the LAT tracker is calculated from the positions of the silicon strips where ionization charge was recorded. The (x, y, z) coordinates of the end of the track correspond to variables called `Tkr1EndPos[0:2]`, and the direction cosines to `Tkr1EndDir[0:2]`. These variables, and many others, including the TimeTone and scaler quantities described in the introduction, are stored in a *Root* file called the *"SVAC tuple"* [16]. It takes about a half-day for the reconstructed data to become available on the SLAC servers.

We extrapolate each muon track to the horizontal plane at the height of the upper muon paddle using

```
XhitHi = Tkr1EndPos[0] + (-Tkr1EndPos[2]+ZPaddleHi)*Tkr1EndDir[0]/Tkr1EndDir[2]
YhitHi = Tkr1EndPos[1] + (-Tkr1EndPos[2]+ZPaddleHi)*Tkr1EndDir[1]/Tkr1EndDir[2]
```

and similarly for the lower paddle. This is done in a *Root* routine called `Output.C` that writes an ascii file with one line per event, each line containing the timing information and the 4 hit positions. The raw timing information is converted to Mission Elapsed Time ("MET") using an algorithm obtained from Anders Borgland at SLAC.

The SVAC tuple files are 1.6 Gbytes for the half-hour muon runs. To gain speed during analysis, only events that hit the paddle level outside of the LAT are kept, and subsequent analysis is performed on these smaller files, using a *Root* routine called `SASS.C`. The routines and ascii data files are available at the Confluence Timing Page.

Figure 4 illustrates the impact points. The exclusion of tracks ending within the LAT volume is apparent, keeping approximately $300,000$ of the initial $880,000$ tracks.

3 Results

Figure 5 summarizes the timing results. Time coincidences are identified as follows: in a first pass through the data, for each VME event index, the LAT event index giving the smallest time difference is tabulated. In a second pass, time differences for all LAT events in a window around that minimum are calculated and plotted. We explored windows from ± 3 to ± 8 events. We require the muon impact points to fall on both the upper and lower muon paddle positions (the small squares in figure 4). The peak at $dT = 24$ ms shown in figure 5 then appears easily. The 3.7 ms width was found to be due to a steady $2.0083\,\mu$s per second clock drift, seen in the top-right frame.

Knowing the 24 ms offset enables us to plot the impact points for coincidence events without the spatial selection, as shown in the right-hand plots of figure 4. The observed paddle positions and those predicted from the geometry layout (table 1 agree well.

Again using the 24 ms offset, we re-tabulated the LAT event indices so as to be able to reduce the window size and thus the background of accidental coincidences. In figure 5 the value used is ± 3 events.

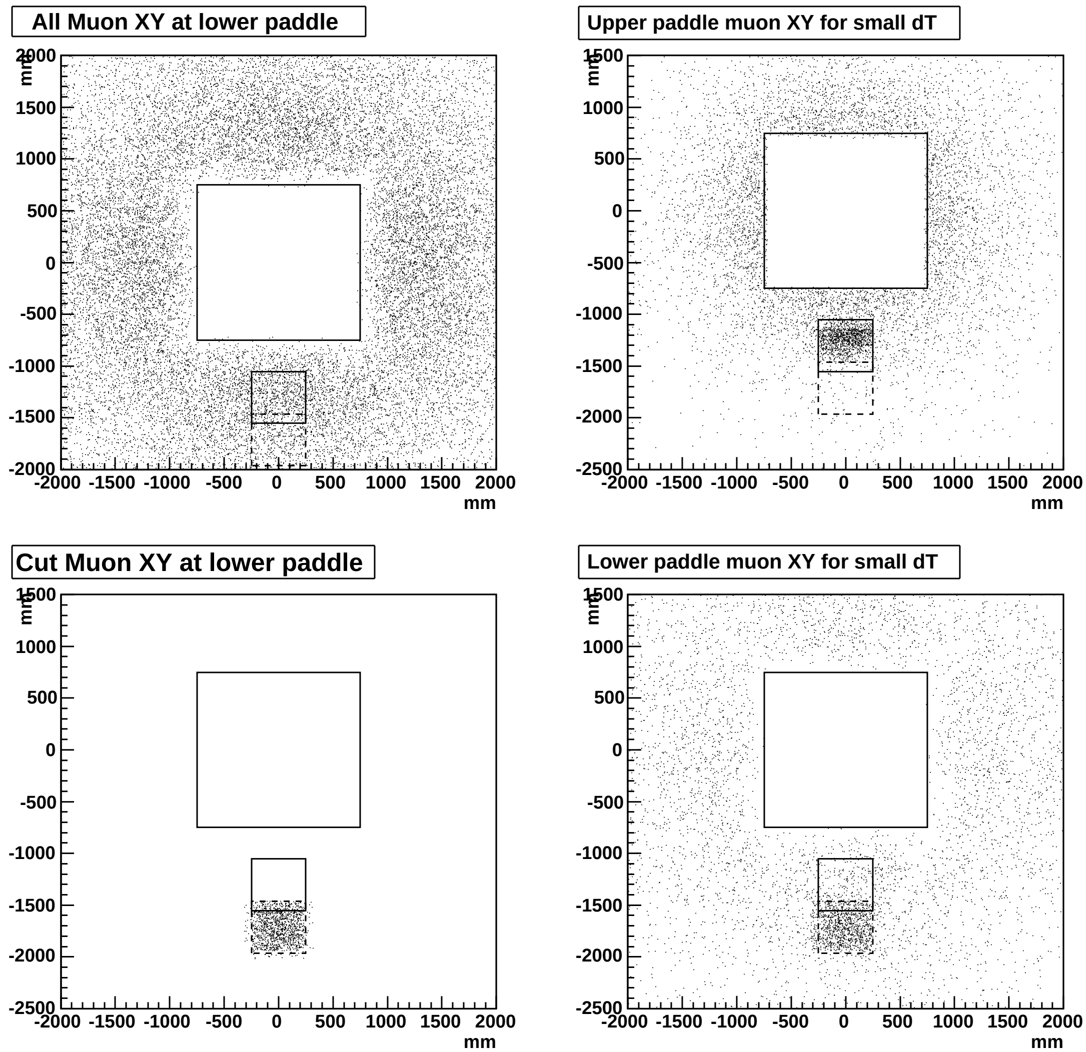

Figure 4: Bird's eye view of extrapolated muon impact points using reconstructed LAT tracks, for run 77013003. The large square is the LAT. The small solid (dashed) square is the upper (lower) scintillator paddle. Top left: In the plane of the lower paddle (i.e., almost on the HiBay floor) for tracks that had already left the LAT volume at the height of the upper paddle. Only 1 in 10 events is shown, for clarity. Top right: Requiring a $20 < dT < 25$ ms time difference between the LAT and the standalone GPS clock, in the upper paddle plane. A clear event excess appears. Bottom right: Same, for lower paddle. Bottom left: Impact points in the plane of the lower panel when the track is required to pass through the upper panel (no timing cut).

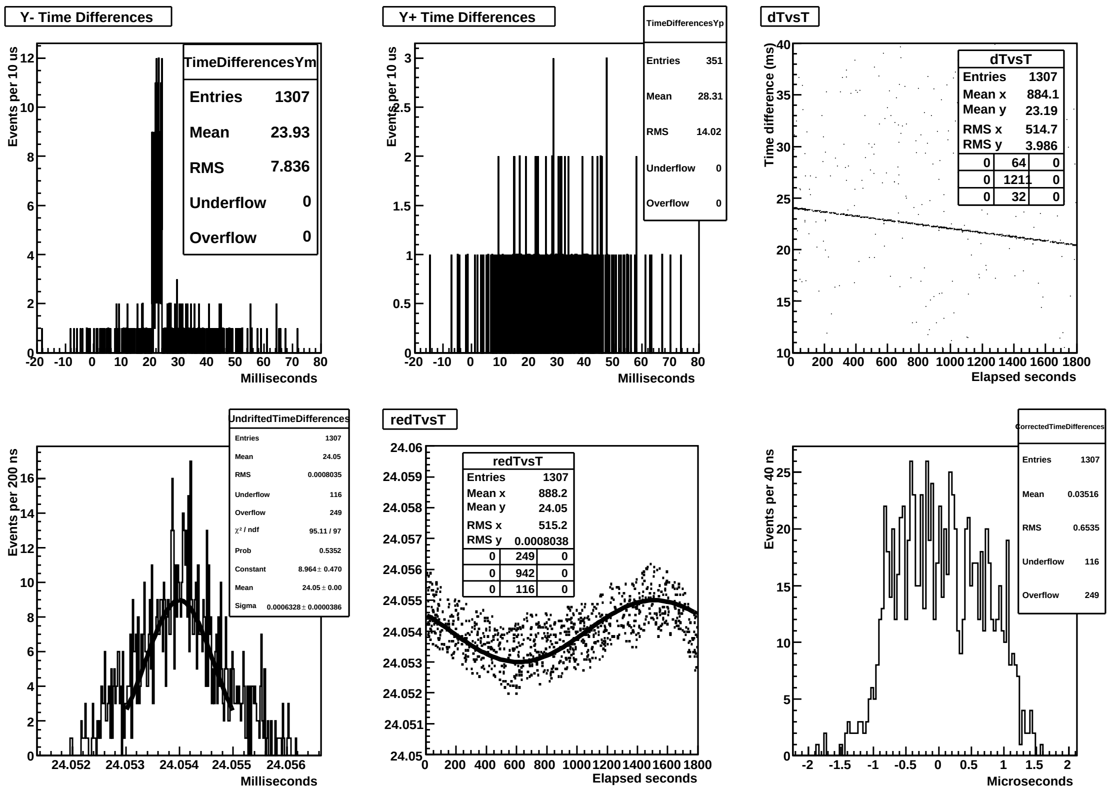

Figure 5: Run 77013003. Top left: Time differences for LAT muon tracks striking both muon scintillators. The spike at $dT \simeq 24$ ms is the signal. The other events are presumably accidental coincidences (see discussion in text). Top middle: same, but for a "virtual" telescope on the opposite side of the LAT. Only accidentals are observed. Top right: dT versus the elapsed time – a steady drift of $2.0083\,\mu$s per second is observed, giving the 3.7 ms width of the peak seen in the top left figure. Bottom left: after subtracting the drift, a gaussian fit yields $\sigma = 0.7\mu$s. Bottom middle: As top right, but after drift subtraction. The 942 coincidence events show a $2\,\mu$s non-linearity. The cosine function to guide the eye is described in the text. Bottom right: After subtracting the cosine function the root-mean-square variance of the distribution is less than 700 ns.

After correcting for the clock drift, the root-mean-square variance of dT distribution is about 700 ns. This is due in part to a $\pm 1\,\mu$s systematic timing drift that nearly sinusoidal with the elapsed time during the data run. The function superimposed on the bottom middle plot is

$$dT = 24.054 + 0.001\cos(1 + 2\pi\frac{T}{1800}),$$

with the elapsed time T in seconds and the time difference dT in milliseconds. In the bottom-right frame we have subtracted this function from measured time differences. The distribution appears roughly uniform between $\pm 1\,\mu$s, surprising given the $0.1\,\mu$s step size of the TTM637 (e.g. figure 3, and the expected precision of our analysis software. We may explore this further.

4 Discussion

A 24 ms offset is surprisingly small when the clock is drifting at 174 ms per day (1.2 s per week). The explanation is that the TimeToneMessage comes from a more accurate clock on the MVME 2304 controlling the VSC crate. That clock is set by the SLAC MCR ("Mobile Computer Rack"), which gets its time from an internet NTP server ("Network Time Protocol"). Typical NTP performance is 5 to 100 ms. The MVME clock get synchronized whenever the VSC is initialized, which occurs only rarely (weeks). The software running in the MVME emits the TimeToneMessage at least 500 ms before the following PPS (see page 93 of [5]). Hence, the drifting PPS hacks a reasonably accurate TimeTone.

The 2.0083 μs per second drift is compatible with the ±30 ppm control range of the undisciplined VCXO in the VSC's TTM637, as described in section 2.2. What of the remaining structure shown in figure 5 (bottom-middle)? The structure shown in figure 3 for the two disciplined GPS's, over only 2 minutes, neither of which was the one actually used at Spectrum, could be interpreted in different ways.

Figure 6 is the result of measurements intended to shed light on the structure. The VSC PPS output was used to trigger the GPS acquisition, in place of the muon telescope. As expected, each event is dated 0.999998 seconds after the preceding event. There is no evidence of the sine-like 4 μs full-width structure seen in figure 5 (bottom-middle). Hence either the muon telescope or the LAT causes the structure. Known muon telescope biases, such as a gain or threshold drift that would cause trigger time-slewing, are at most a few tens of ns and seem unlikely to produce the observed structures. Figure 6 does show some drifts at the sub-100 ns level: on timescales of an hour or more, the $-2.2\,\mu$s population grows or shrinks at the expense or gain of the $-2.1\,\mu$s population. Such an effect could be explained by the changing constellations of GPS satellites being picked up, and in any case is small compared to the GLAST science requirements.

5 Discussion

Random ("accidental") time coincidences between a muon having triggered the LAT and a different one tagged by the paddles populate the top-middle plot of figure 5. There are 351 events for this choice of analysis parameters (subtraction of the 24 ms offset, and a ±3 event window). The two bottom plots show 942 events in the signal, with no apparent background contamination. (942 + 351) = 1293 events agrees surprisingly well with the 1307 events in the top-left plot, considering the expected statistical fluctuation of $\pm\sqrt{351} = \pm 19$ events. This leads us to believe that the outlying events in the top-left plot are indeed accidental background, and in particular that there is no evidence of occasional mistimed events in our data.

Before any timing cuts, 2320 tracks pass through both paddle positions. The fraction with telescope time tags is $\epsilon = 942/2320 = 0.41$, suggesting that the efficiency of each of the four PMT's is $0.41^{1/4} = 80\%$. This is plausible in light of discriminator settings adjusted well above the electronics noise level.

6 Prospects

We now consider preparations for the test with the real spacecraft. After integration, the top of the LAT will be 3429 mm above the floor, and the observatory will be on a stand 1880 mm wide [17]. Figure 7 illustrates the muon telescope geometry for three different telescope positions. Applying this geometry to data run 77013003 and requiring that the muon track pass through both the top and bottom scintillator paddles, we predict that 4222, 2926, and 1271 tracks would traverse the paddles for the 3 layouts shown in the figure, respectively. Normalizing to the ratio 942/2320 discussed above, we predict 1731 coincidences if we again unbolt the top paddle and move it closer to the LAT, as shown in the leftmost figure.

The other aspect is to foresee ancillary measurements that we'll make during the tests. Here is a preliminary list:

1. Two TTM637's will be available at Spectrum: the one from the spare VSC, and the one from SLAC loaned to Bordeaux in preparation for the proof-of-principle tests. We can thus repeat the measurement shown in figure 3, although using only a single GPS antenna via a signal splitter. We will ask Alan Ames of Spectrum Astro to provide us with this splitter. We would do this with a longer timebase, repeated several times over a few days.

2. If a PPS output from the spacecraft is available, we can use it to latch times in the standalone VME GPS and thus get an independent determination of the PPS clock rate, as shown for the VSC in figure 6.

3. In case some unexpected timing behavior is observed, we need to know what if any diagnostic information is available from the spacecraft, analogous to the various flags and scaler values output by the LAT.

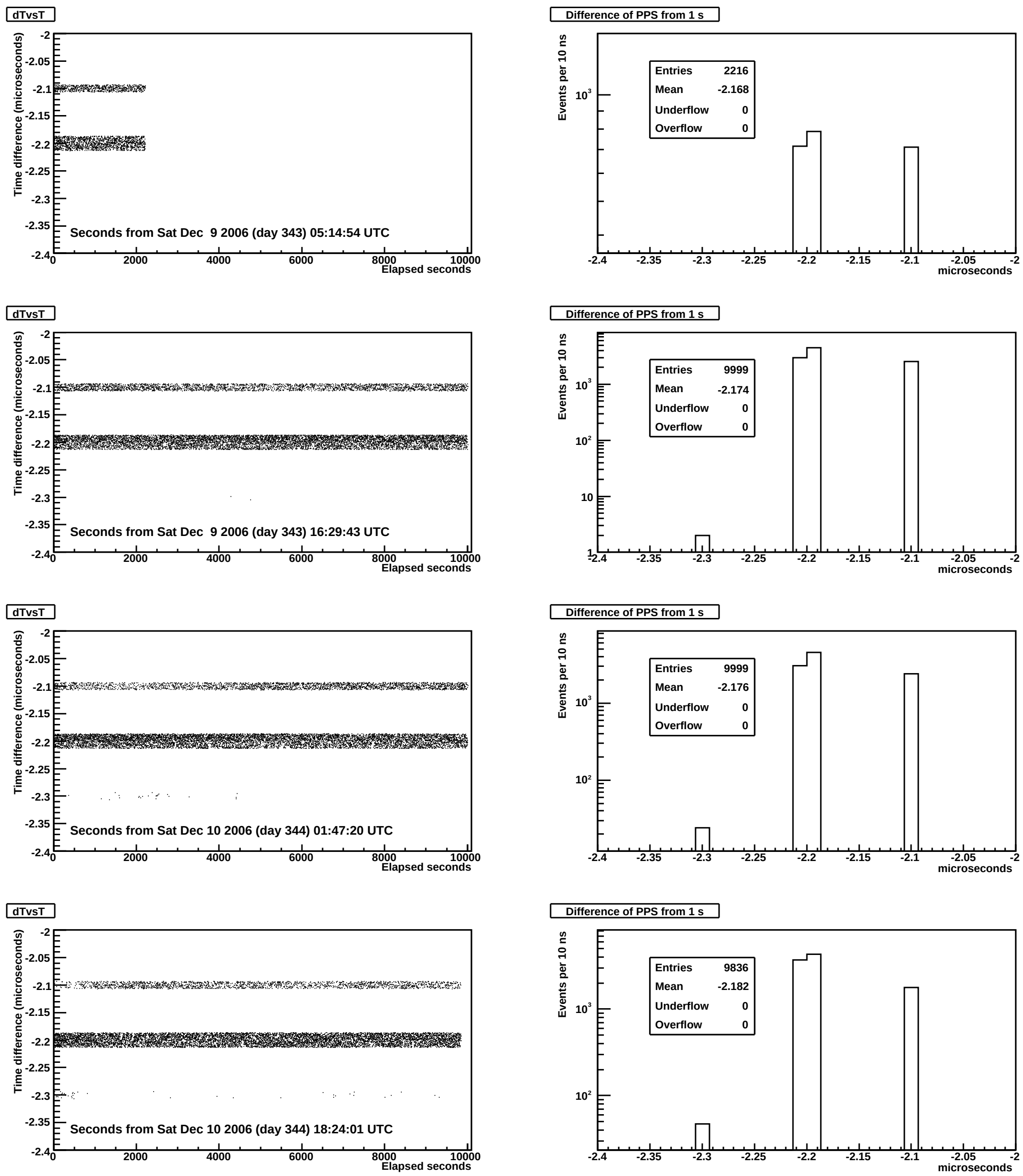

Figure 6: Results of a check of the VSC and GPS performance. The VSC PPS was used to latch the VME GPS times, in place of the muon telescope trigger. A half-hour run, then three 3-hours runs were acquired. One second is substracted from the time that elapsed between two successive triggers, and the $-2.0083\,\mu$s drift appears rounded to the following least significant tick, i.e. to $-2.1\,\mu$s for roughly a third of the events, and to $-2.2\,\mu$s for most of the rest. Occasionally, $-2.3\,\mu$s appears. An oscillation of less than 100 ns amplitude can be (faintly) seen on a $\sim$hour timescale.

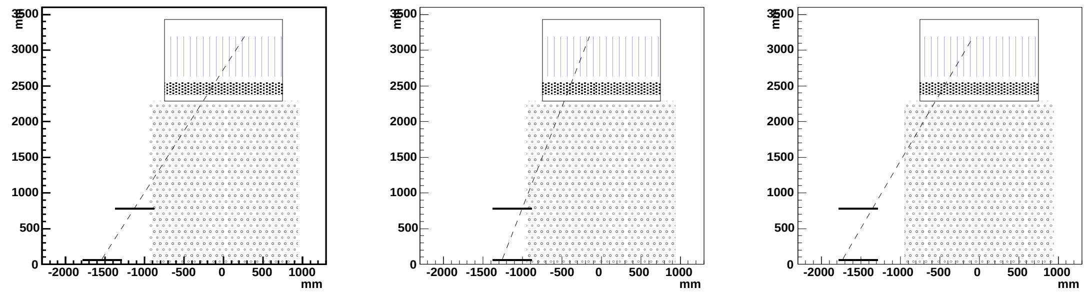

Figure 7: LAT integrated with spacecraft, mounted on stand. Left: top scintillator unbolted from the stand and moved closer to LAT, as in November tests. Middle: Both scintillators unbolted and moved closer. Right: Both paddles fixed in original position on stand. The dashed lines illustrate muon tracks striking the scintillator edges at $\frac{1}{2}$, $\frac{1}{4}$ and $\frac{1}{8}$ of the paddle width from the paddle edge, respectively, for the 3 frames.

In conclusion: we have demonstrated the validity of the absolute timing end-to-end test scheme, and we are ready to proceed with the real test on the spacecraft once the flight CD&H system and the LAT have been integrated.

Acknowledgements: Thanks to Neil Johnson and Dave Thompson for encouraging the proposition, and to Neil Johnson for getting the tests approved. Ron Zitek and Alan Ames of Spectrum Astro provided key on-site support. Thanks to Patty Sandora for her work on the muon telescope, as well as to Gregg Thayer for discussions, and for the loan of the SLAC TTM637.

References

[1] Thompson, D.J. "Future Gamma-Ray Observations of Pulsars and their Environments", to appear in proc. 363^{rd} Heraeus Seminar, May 2006, `http://www.mpe.mpg.de/363-heraeus-seminar/`. See also astro-ph/0312272.

[2] "Science Requirements Document", `http://glast.gsfc.nasa.gov/science/433-SRD-0001_CH-03.pdf`

[3] "LAT Instrument-Spacecraft Interface Requirements Document", `http://giants.stanford.edu/ioc/docs/433-IRD-0001.pdf`

[4] LAT-SS-00010 "LAT Level II(B) Performance Specification". See also tests LAT 13x described in section 6.7.2.10 the "Performance and Operation Test Plan" LAT-MD-02730-04.

[5] The Virtual Spacecraft User's Manual, LAT-TD-05601.

[6] `http://confluence.slac.stanford.edu/display/CAL/Event+Timestamps`

[7] S. Murray et al, ApJ 568, 226-231 (2002)

[8] Kirsch, M.G.F. et al, Proc. SPIE 5165, 85-95 (2004).

[9] `http://pdg.lbl.gov/2006/reviews/cosmicrayrpp.pdf`.

[10] Scintillator frame assembly LAT-DS-03971.

[11] Transport container base assembly LAT-DS-07556 and pallet frame LAT-DS-07553.

[12] Thanks to A. Moissev for leading us to LAT-DS-00038, which shows the LAT z-orgin to be 236.2 mm above the LAT interface to the spacecraft, and the extreme top to be 1050 mm above the interface.

[13] LAT Instrument Data Analysis Primer, `http://www-glast.slac.stanford.edu/IntegrationTest/SVAC/Instrument_Analysis/UsefulStuff/LAT-TD-04631-02.htm`

[14] de Naurois, M., Holder, J. et al., ApJ 566, 343-357 (2002)

[15] Symmetricom TTM637VME Time and Frequency Processor User's Guide.

[16] SVAC root file formats are described at http://www-glast.slac.stanford.edu/IntegrationTest/SVAC/Instrument_Analysis/Instrument_Analysis.html.

[17] Power point sketch of LAT post-integration geometry prepared by Marc Campell.